ELSEVIER

Chemical Engineering Journal 136 (2008) 92–98

Chemical Engineering Journal

www.elsevier.com/locate/cej

Kinetic sorption of Cr(VI) into solvent impregnated porous microspheres

Cristian O. Illanes, Nelio A. Ochoa*, Jose Marchese

Laboratorio de Ciencias de Superficies y Medios Porosos, Universidad Nacional de San Luis-FONCYT-CONICET, Chacabuco 917, San Luis, Argentina

Received 22 December 2006; received in revised form 7 February 2007; accepted 2 March 2007

Abstract

The sorption rates of Cr(VI) ion from acid chromate solutions with Aliquat 336 impregnated microspheres (MS) were examined. MS of polysulfone (PSf) and poly(styrene-acrylenitrile) (SAN) were prepared by phase inversion process. The MS obtained have different size and morphology. The sorption behavior and the rate-controlling sorption step have been discussed from the Elovich equation, pseudo-second order and Crank kinetic models. Even all models gave satisfactory correlations with the experimental data, the Crank model showed to be more realistic and appropriate to interpret the Cr(VI) kinetic sorption results. These analysis indicate that the intraparticle solute diffusion is the rate-controlling sorption step, and suggest that there is a surface diffusion contribution to the overall Cr(VI) mass transport inside the MS which is more important as the MS pore size decreases.

Keywords: Microspheres; Cr(VI) sorption; Kinetics

1. Introduction

In a recent work, we reported the microspheres (MS) preparation by the inversion phase technique from polysulfone and polyvinylpirrolidone [1]. This procedure has the advantage that appropriate porous supports to be used in solvent extractant impregnation can be prepared from available commercial polymers. Both, the extractant chemical characteristics and operational conditions of feed aqueous solution will determine the ion to be recovered. This separation technique using solvent impregnated resins SIR [2–6] is similar to the one reported by other researchers, which is used as an alternative method to the of ions extraction by solvents. Recently, metallic ion separation with microcapsules (MC) using alkylphosphoric acids [7–9] and quaternary ammonium salts [10] has been reported. These ion extraction techniques (MS, SIR, and MC) have a similar extraction procedure that is, the ions are extracted by the extractant liquid phase immobilized into the porous structure or cavities of the support.

Although in the literature different kinetic models to interpret the ion sorption mechanisms on the heterogeneous liquid–solid phase have been proposed, two models have been mainly used to determine the main step in the ion sorption process: the homogeneous diffusion model (HDM) based on Fick's law, and the shrinking core model (SCM) [11]. In the first case, two main steps are considered: the ion diffusion through the stagnant liquid layer and in the particle. In the second model, three mechanisms are proposed: diffusion through the stagnant liquid layer, diffusion in the particle and chemical reaction [10,12]. Cortina and Miralles [12] studied the extraction kinetic of Cd(II), Cu(II) and Zn(II) ions using di(2,4,4-trimethylpentyl)phosphinic acid—XAD2 resin. They found out that at high metallic ionic concentration the main step on ion extraction was the diffusion in the resin phase. When low ion concentration was used, the determinant extraction rate step was the ion diffusion through the stagnant film.

Juang and Chen [13] analyzed the sorption rate of Fe(III), Co(II), Ni(II), Cu(II) and Zn(II) ions with macroporous resins containing bis(2-ethylhexyl) phosphoric acid (D2EHPA) as extractant. Their experimental data were not adequately fitted with the HDM and SCM models, while using the Elovich equation, a good data correlation was obtained. The sorption mechanism of these metallic ions was discussed according to

* Corresponding author. Tel.: +54 2652 424689; fax: +54 2652 430224.
E-mail address: aochoa@unsl.edu.ar (N.A. Ochoa).

1385-8947/$ – see front matter © 2007 Elsevier B.V. All rights reserved.
doi:10.1016/j.cej.2007.03.008

the activation energy values. At high metallic ions concentration, within the experimental time range studied, the ion diffusion in the particle played a dominant role on the sorption rate. The Elovich's equation has been widely used to study the adsorption kinetic of gases on solid surfaces [14]. This equation has been also applied to describe the adsorption in aqueous media of both phosphate and arsenic species on goethite [15,16]. Juang and Chou [17] found out that sorption kinetics of citric acid from aqueous solutions by macroporous resins containing a tertiary amine can be adequately interpreted by the Elovich equation.

Kamio et al. [9] studied the sorption behavior of Ga(III) and In(III) ions in MS containing 2-ethylhexylphosphonic acid mono 2-ethylhexyl ester. The sorption mechanism was evaluated from activation energy data. The activation energy values for sorption indicated that diffusion and chemical reaction steps controlled ion sorption rates.

The aim of this study is to measure and compare the sorption rate of Cr(VI) ion from acid chromate solutions with Aliquat 336 impregnated microspheres. This extractant is an effective compound to remove Cr(VI) from industrial effluents and is widely used in liquid–liquid extraction process [18]. The effect of MS morphology on the ion sorption kinetics will be analyzed. The sorption behavior and the mainly controlling sorption steps will be discussed according to kinetic models, such as: Elovich equation, pseudo-second order and Crank models.

2. Experimental

2.1. Reagents

Polysulfone P-3500 (PSf) was provided by Amoco, poly (styrene-co-acrylonitrile) was provided by Bayer. AG polyvinylpyrrolidone K30 and sodium dodecyl sulfate were purchased from Fluka, Aliquat 336 was supplied by Cognis. Agar–agar powder, dichloromethane (DCM), potassium dichromate and chromium standard for AA (titrisol) were provided by Merck.

2.2. Microsphere preparation

Precursor polymeric solution consists of a mixture of different ratios of PSf and PVP. PSf is a linear polymer soluble in DCM and insoluble in water while PVP is a polymer soluble in DCM as well as in water. In this route, MS formation occurs by phase inversion process of PSf polymer, while the presence of PVP favors the generation of cavities or pores in MS structure. PSf–PVP mixture was varied according to the following weight ratios: 1:1, 2:1, and 1:3. A detailed composition of precursor solutions is shown in Table 1.

The experimental methodology of MS synthesis is based on the following outline: in a 1 dm^3 vessel, 0.8 dm^3 of distilled water with 2% agar–agar and 2% sodium dodecyl sulfate were added. The polymeric solution was added dropwise to the aqueous phase under continuous mixing with a blade stirrer (800 rpm). After the last drop was added, emulsion temperature was gradually increased up to 50 °C. Finally, MS were filtered, washed with distilled water and air-dried at room temperature.

Table 1
Composition of polymer solutions

	Polymer (wt.%)	PVP (wt.%)	DCM (wt.%)
PSf–PVP 1:1	11.62	11.62	76.75
PSf–PVP 2:1	12.34	6.17	81.49
PSf–PVP 1:3	7.55	22.65	69.80
SAN–PVP 1:1	11.62	11.62	76.75
SAN–PVP 2:1	12.34	6.17	81.49
SAN–PVP 1:3	7.55	22.65	69.80

The same procedure for SAN–PVP microspheres preparation was carried out.

2.3. Microsphere impregnation and batch sorption experiments

MS samples were impregnated in solution of Aliquat 336, a selective extractant of ion Cr(VI). Impregnation was performed by the following methodology: 0.33 g of MS was put into contact with 1 g Aliquat 336 for 24 h. Impregnated MS (IMS) were separated by filtration from the excess of extractant solution and washed three times with distilled water. Extraction batch tests at 298 K were carried out. Extraction procedure consisted in placing 0.3 g of IMS in contact with 80 cm^3 of 40 ppm Cr(VI) ion aqueous solution at pH 4. During extraction tests, solutions in contact with MS were constantly stirred at 100 rpm and samples of aqueous solutions were taken at different intervals. The Cr(VI) concentration was determined by atomic adsorption spectrometry using a Varian 50AA spectrometer. Aliquat 336 final content in the MS was determined by change of weight before and after heptane extraction.

2.4. Characterization

2.4.1. Scanning electron microscopy

SEM images were obtained using a Carl Zeiss microscope. Microsphere samples were coated by sputtering a thin gold layer. They were observed under high vacuum. Figs. 1 and 2 show the

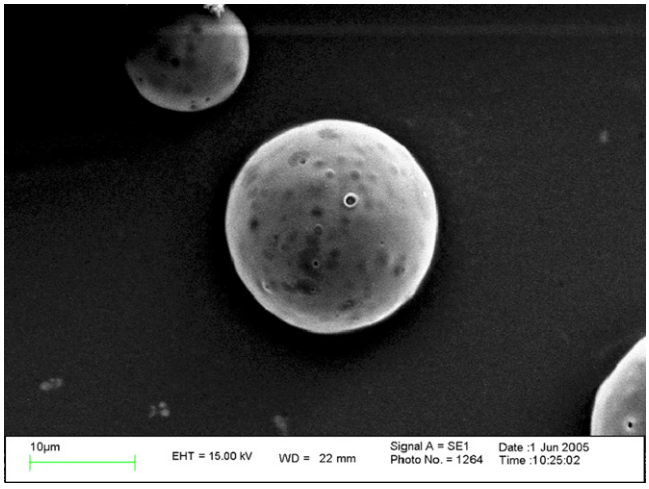

Fig. 1. Microphotograph of PSf 2–1 MS.

Table 2
MS structural parameters from Hg intrusion and SEM images

Microspheres	PSf–PVP 2:1	PSf–PVP 1:1	PSf–PVP 1:3	SAN–PVP 2:1	SAN–PVP 1:1	SAN–PVP 1:3
Total intrusion volume (mL/g)	0.3566	0.4855	0.2147	0.9158	0.3446	0.0430
Average pore diameter ($4V/A$) (μm)	0.1243	0.3238	0.0121	0.0406	0.0165	0.0215
Porosity (%)	14.705	17.602	13.266	29.269	25.500	13.151
Particle diameter (μm) (SEM)	18	120	30	25	333	150

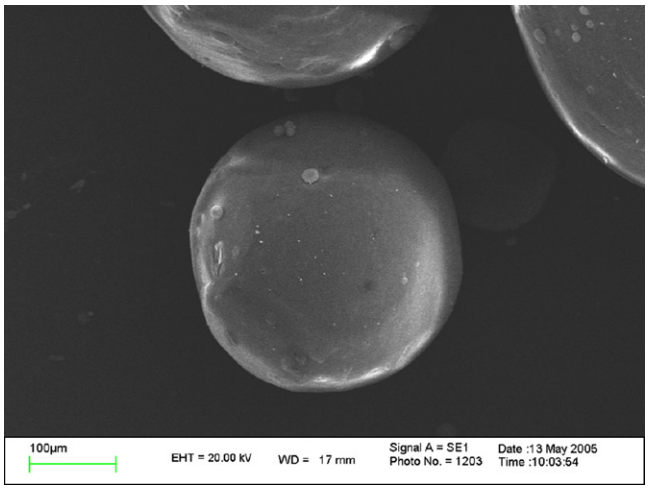

Fig. 2. Microphotograph of SAN 1–1 MS.

micrograph of PSf–PVP 2:1 and SAN–PVP 1:1. The particle size distribution and mean particle size were determined using an image analyzer. Table 2 shows the mean particle sizes obtained from this analysis.

2.4.2. Hg porosimetry

MS pore size distribution, mean pore diameter and porosity were studied with an Autopore III 9410 Micromeritics Porometer. Table 2 shows the MS structural parameter values.

The effect of operational parameters on the ME structural characteristics has been discussed in previous work [1].

3. Sorption mechanisms

3.1. Elovich equation

The Elovich equation is given by:

$$\frac{dq}{dt} = A\, e^{(-\alpha q)} \tag{1}$$

where q (mol Cr/g MS) is the amount of solute adsorbed at time t (s), A (mol/g s) and α (g/mol) are constant. The parameter A can be considered as the initial rate since $(dq/dt) \to A$ as $q \to 0$. It has extensively been accepted that the chemisorption process can be described by this semi-empirical equation. Zhang and Stanforth [16], by quotation from Parravano and Boudart's work [19], mentioned that the Elovich equation allows to establish if the process is based on diffusion or chemical reaction control. When the adsorption is based on energetically heterogeneous surface, the parameter α is related to the distribution of activation energies. In the diffusion control model, α is a function of both the particle structural–chemical characteristics and solute diffusion coefficient. Pavlatou and Polyzopoulos [20] suggested that the conformity of Elovich equation may only be taken as evidence that the rate-controlling step is the solute diffusion. Aharoni et al. [21] also suggested that diffusion accounted for the Elovich kinetic patterns.

3.2. The kinetic model of pseudo-second order

Ho and McKay [22] developed the pseudo-second order kinetic model where the chemisorption equation is represented by:

$$\frac{dq}{dt} = k_2(q_e - q_t)^2 \tag{2a}$$

where, in our chromium-microspheres system, k_2 is the pseudo-second order rate constant for sorption (mol/g s), q_e and q_t are the chromium sorbed at equilibrium and at time t, respectively. Arranging Eq. (2a) and integrating (with $q = 0$ at $t = 0$ and $q = q$ at $t = t$) the following expression is obtained:

$$\frac{1}{(q_e - q)} = \frac{1}{q_e} + kt \tag{2b}$$

Eq. (2b) can be rearranged to obtain a linear form:

$$\frac{t}{q} = \frac{1}{k_2 q_e^2} + \frac{t}{q_e} \tag{3}$$

3.3. Crank model

In their kinetic data interpretation, Matthews and Weber [23] and Choy and McKay [24], used the diffusion model proposed by Crank [25]. In their analysis, the mass-transfer rate, N_t, at the external surface of MS is given by:

$$N_t = \frac{\partial C_t}{\partial t} = k_i S_A (C_{(t)} - C_s) \tag{4}$$

where C_s is the liquid phase concentration at the surface in equilibrium with the solid-phase concentration, q, k_i the external mass-transfer coefficient (m/s) and S_A is the specific surface area of sorbent:

$$S_A = \frac{6m_s}{d_p \rho_s} \tag{5}$$

where m_s is the solid-phase concentration in liquid phase (kg), d_p the particle diameter (m), and ρ_s is the skeletal density of microsphere (kg/m^3).

The external mass-transfer coefficient can be directly calculated by the film diffusion equation proposed by Matthews and Weber [23]:

$$\ln\left(\frac{C_{(t)}}{C_0}\right) = -k_i S_A t \tag{6}$$

when $t \to 0$ and $C_s \to 0$.

According to Crank diffusion model [25], the concentration of solute (q) inside microsphere at distance r, from the centre and at time t, is governed by the following diffusion equation:

$$N_t = \frac{\partial q}{\partial t} = \frac{D_{app}}{r^2}\frac{\partial}{\partial r}\left[r^2\frac{\partial q}{\partial r}\right] \tag{7}$$

where D_{app} is the apparent diffusion coefficient (m^2/s) of the sorbent in the particle.

For the two resistances model, external film mass transport and intraparticle diffusion, the differential equation solution proposed by Crank is:

$$D_{app}\left.\frac{\partial q}{\partial r}\right|_r = k_i S_A(C_e - C_s) = k_i S_A m_s(q_e - q_s|_r) \tag{8}$$

where C_s is the liquid phase concentration at the surface in equilibrium with the solid-phase concentration $q|_r$. The final equilibrium concentration in the bulk liquid phase is C_e and q_e is the equilibrium solid-phase concentration.

For a step change in the bulk concentration from C_0 to C_e at $t = 0$, the solution for the uptake curve is:

$$\frac{\bar{q} - q_0}{q_e - q_0} = 1 - \sum_{n=1}^{\infty}\frac{6L^2\exp(-\beta^2 D_{app}t/r_p^2)}{\beta_n^2[\beta_n^2 + L(L-1)]} \tag{9}$$

where $\bar{q}$ is an average solid-phase concentration of the particle; q_0 is an initial mean equilibrium solid-phase concentration;

$$L = \frac{k_i r_p m_s}{D_{app}} \tag{10}$$

and β_n represents the roots of the equation:

$$\beta_n \cot\beta_n + L - 1 = 0 \tag{11}$$

Eqs. (6) and (8)–(11) have been solved for each experiment and best-fit mass-transfer coefficients and diffusivities, k_i and D_{app}, have been obtained.

4. Results and discussion

4.1. Elovich equation

Experimental data of chromium absorption were analyzed with the Elovich equation. The dq/dt versus q values are shown in Figs. 3 and 4. Solid lines indicate the data fit obtained with the Levenberg–Marquardt minimization method (chi-square). Fitting parameters are given in Table 3.

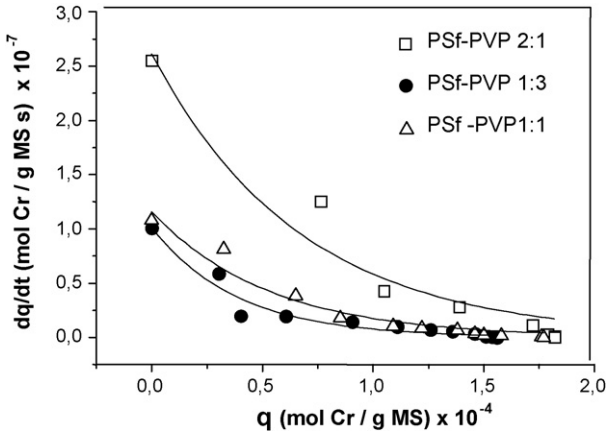

Fig. 3. Elovich equation PSf-MS. Experimental points (symbols), fitting curve (solid curve).

Table 3
Elovich equation's parameters

Microspheres	A ($\times 10^8$ mol/g s)	α ($\times 10^{-4}$ g/mol)	χ^2
PSf–PVP 2:1	26.155 ± 2.151	1.499 ± 0.201	4.7077E−16
PSf–PVP 1:1	11.586 ± 0.686	1.889 ± 0.171	5.2871E−17
PSf–PVP 1:3	10.117 ± 0.639	2.590 ± 0.272	4.3404E−17
SAN–PVP 2:1	8.355 ± 0.807	4.663 ± 0.684	6.6407E−17
SAN–PVP 1:1	7.882 ± 0.383	3.056 ± 0.246	1.5920E−17
SAN–PVP 1:3	4.231 ± 0.343	8.281 ± 1.091	1.2069E−17

Juang and Chen [13] found out that the parameter A of the Elovich equation reached a maximum value when it is represented in a log–log plot versus the metallic ion concentration extracted with D2EHPA (Zn (II), Fe(III) and Cu(II) in aqueous phase). These authors also reported that higher initial sorption rates give smaller α values. Table 3 data corroborated this last tendency in contrast with gas–solid chemisorptions systems reported by other authors [26,27].

4.2. Kinetic model of pseudo-second order

Figs. 5 and 6 show the experimental data representation of t/q versus t (Eq. (3)). The pseudo-second order constant (k_2), the

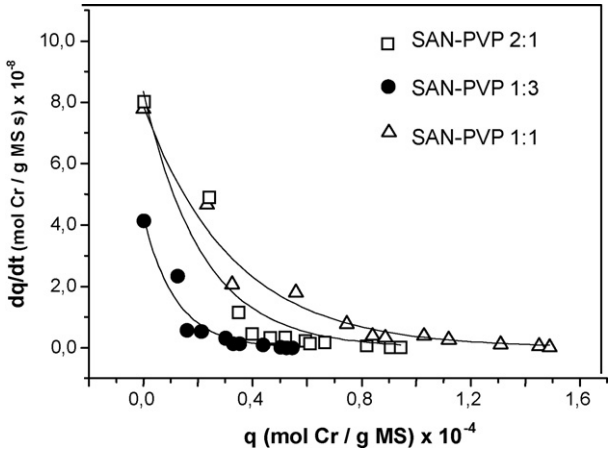

Fig. 4. Elovich equation in SAN-MS. Experimental points (symbols), fitting curve (solid curve).

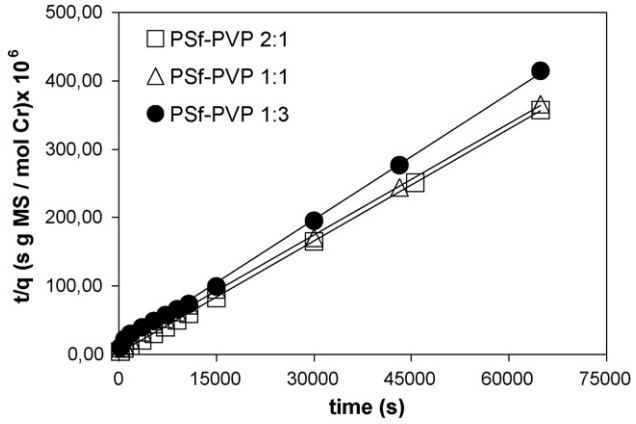

Fig. 5. t/q vs. t in PSf-MS. Experimental points (symbols), pseudo-second order model (—).

Table 4
Parameters for pseudo kinetic second order model

Microspheres	k_2 (mol/g s)	q (mol Cr/g MS)	$t_{1/2}$ (s)	R^2
PSf–PVP 2:1	21.30	1.82E−4	257.96	0.9989
PSf–PVP 1:1	2.55	1.77E−4	2215.58	0.9900
PSf–PVP 1:3	2.94	1.56E−4	2180.36	0.9989
SAN–PVP 2:1	2.65	1.34E−4	2816.11	0.9944
SAN–PVP 1:1	1.54	1.49E−4	4358.06	0.9970
SAN–PVP 1:3	5.78	5.45E−5	3174.50	0.9984

absorption concentration at equilibrium (q_e) and the initial sorption rate ($k_2 q_e^2$) calculated by fitting the straight lines of these plots are summarized in Table 4. A good correlation coefficient from the linear regression was achieved ($R^2 > 0.99$).

In Table 4 the half sorption time ($t_{1/2}$) has been included. This is defined as the required time to uptake the half of the maximum amount of sorbed Cr(VI) at equilibrium. The half-sorption time also characterize the sorption process. It can be observed from Tables 4 and 2 that for microspheres with lower diameter size (PSf–PVP 2:1 and SAN–PVP 2:1) the lowest half sorption time is obtained. These results indicate that when the particle size is increased, the sorption process will occur more slowly. It can be

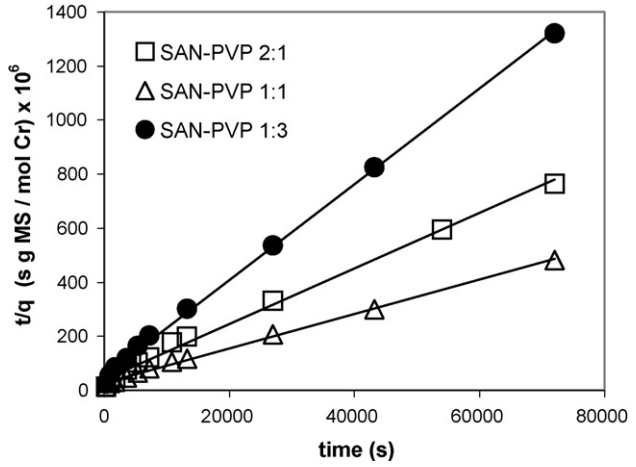

Fig. 6. t/q vs. t in SAN-MS. Experimental points (symbols), pseudo-second order model (—).

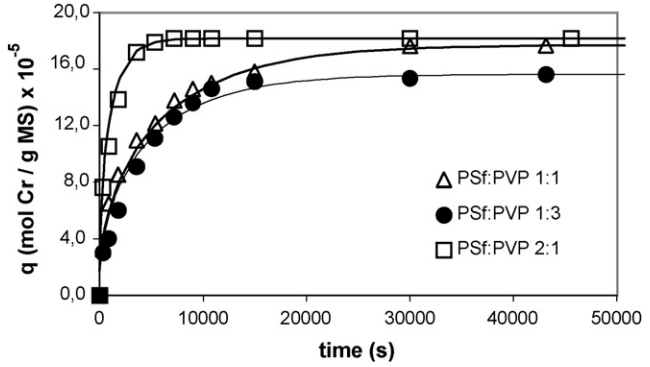

Fig. 7. Cr(VI) sorption vs. t in PSf-MS. Experimental points (symbols), Crank model (solid curve).

also observed that when the lower the particle size is, the greater equilibrium concentration of Cr(VI) is reached.

4.3. Crank model

To illustrate the ability of Crank model to characterize the experimental data, sorption kinetics plots are represented in Figs. 7 and 8. These results show the good correlation between the theoretical (solid lines) and experimental values of Cr(VI) sorption in the MS.

The Crank parameters (k_i and D_{app}) for sorption kinetics of Cr(VI) calculated by fitting the experimental data with Eqs. (6) and (8)–(11) are summarized in Table 5.

Biot's number allows distinguishing if the sorption process is controlled by the mass transport in the particle external boundary layer or by the Cr–Aliquat 336 complex diffusion inside the pore, according to the following expression

$$\text{Biot} = \frac{k_i r_p}{D_{app}} \tag{12}$$

where r_p is the particle radius. A Biot's number higher than one indicates that, the complex diffusion through the particle pore is the controlling transport step. When Biot $\ll 1$, the external mass transfer becomes the predominant mechanism. Biot numbers calculated with parameters obtained from the sorption kinetics model are given in Table 5. These Biot number values ($\gg 1$) suggest that the sorption process is mainly

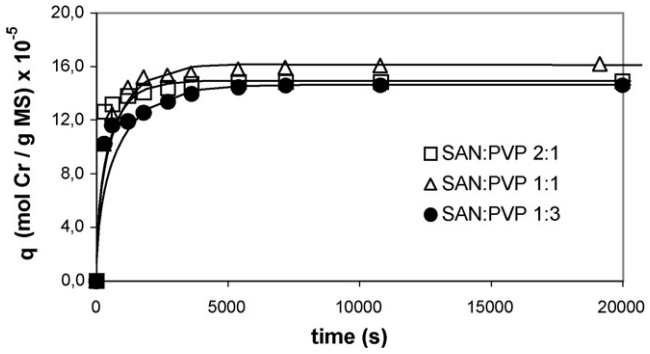

Fig. 8. Cr(VI) sorption vs. t in SAN-MS. Experimental points (symbols), Crank model (solid curve).

Table 5
Kinetics data from Crank model, Langmuir isotherm, and surface diffusion

Microspheres	k_i ($\times 10^7$ m/s)	D_{app} (m^2/s)	Biot	*Re*	K_L (L/g)	a_L ($\times 10^{-4}$ L/mol)	R^2_{La}	D_{eff} (m^2/s)	D_s (m^2/s)
PSf–PVP 2:1	1.89	6.0×10^{-15}	288	12.14	5.8431	3.01	0.90	7.2×10^{-16}	6.4×10^{-20}
PSf–PVP 1:1	3.60	4.5×10^{-14}	477	147.5	1.3910	4.22	0.96	1.1×10^{-15}	3.0×10^{-18}
PSf–PVP 1:3	1.23	3.5×10^{-15}	527	23.36	25.0618	69.4	0.99	5.8×10^{-16}	3.9×10^{-19}
SAN–PVP 2:1	0.84	2.2×10^{-14}	46	18.32	0.1918	1.00	0.98	7.7×10^{-16}	2.7×10^{-17}
SAN–PVP 1:1	50.60	2.0×10^{-12}	281	580.88	2.7334	8.40	0.99	3.4×10^{-15}	0.5×10^{-15}
SAN–PVP 1:3	13.30	4.7×10^{-13}	212	203.33	0.3422	0.79	0.97	2.4×10^{-15}	0.6×10^{-15}

controlled by the intraparticle diffusion. Saha et al. [28] in their extraction experiments with SIR founded diffusion coefficients, D_{app}, for Cr(VI) sorption for all samples lie in the range $(4.28–11.90) \times 10^{-12}$ m^2/s by assuming a intraparticle diffusion control governed by Fick's second law. Their SIR were formed by impregnating Amberlite XAD-7 with Aliquat 336 as the extractant at pH 6.

Furusawa and Smith [29] have established that the Reynolds number (*Re*) of sorbent particles can be defined as

$$Re = \left(\frac{\in d_p^4}{\nu^3} \right)^{1/3} \tag{13}$$

where $\in$ is the energy dissipation rate per unit mass of particle-free liquid, ergs/(g s), which is a function of potential number and the impeller both rpm and geometry [29]; and ν the kinematic viscosity. It can be noted from this equation that keeping the same particle stirring, the *Re* number increases with the particle diameter, which in turn produces an increase in the mass-transfer coefficient. It can be noted from Table 5 that the mass-transfer coefficient follows the expected trends, as far as they increase with the MS diameter.

If we compare the Cr–Aliquat complex diffusion coefficients obtained from Crank Model with the free diffusion coefficient $\bar{D} = 1.15 \times 10^{-13}$ m^2/s calculated from the semiempirical expression given by Wilke-Chang [30], it can be seen that D_{app} in SAN–PVP 1:1 and 1:3 MS are much larger than $\bar{D}$. Furusawa and Smith [29] account from this behavior by considering that there is (exist) a surface diffusion of the solute which is described as a surface migration or hopping between adjacent sites of different adsorption strength. Several researchers [31–34] have also explained their experimental data of solute diffusion through gel microporous resins considering this surface migration mechanisms.

To account this surface diffusion contribution Furusawa and Smith [29] found out the following relation

$$D_{app} = D_{eff} + \frac{\rho_p K_L D_s}{\varepsilon} \tag{14}$$

where D_s is the surface diffusivity (m^2/s), D_{eff} the effective diffusion coefficient inside of the pore, ρ_p the particle density, ε the solid porosity, and K_L is the Langmuir adsorption equilibrium constant (m^3/kg). D_{eff} can be calculated by [35]:

$$D_{eff} = \frac{\varepsilon \bar{D}}{\tau} \tag{15}$$

with

$$\tau = \frac{(2-\varepsilon)^2}{\varepsilon} \tag{16}$$

where τ is the solid tortuosity.

The Langmuir isotherm for solute sorption can be expressed as [9]:

$$q = \frac{K_L C}{1 + a_L C} \tag{17}$$

where a_L is a constant in Langmuir isotherm, L/mol, K_L the adsorption equilibrium constant, L/g of MS, and C is the Cr(VI) bulk concentration at equilibrium (mol/L).

The Langmuir parameters (K_L, a_L) obtained by fitting our experimental data of absorbed Cr(VI) concentration in the MS versus Cr(VI) concentration at equilibrium in the bulk solution (Eq. (14)), and D_{eff} and D_s data obtained from Eqs. (14)–(16) are shown in Table 5. The good correlation between the theoretical Langmuir isotherm and experimental data, given by the correlation coefficient R^2_L, suggests that this sorption mechanisms is adequate to interpret the of Cr(VI) sorption at equilibrium with MS.

From these results the D_{eff} and D_s values can be compared. They show clearly that the surface diffusion coefficient increases as the microsphere pore size decreases. When Cr(VI) sorption is carry out with PSf–PVP and with SAN–PVP 2:1 microspheres, the surface diffusion contribution is negligible compared with the effective diffusion transport ($D_{eff} \gg D_s$). On the other hand, in the Cr(VI) sorption process with SAN–PVP 1:1 and 1:3 MS the solute surface diffusion contribution becomes more important (D_s of the same order than D_{eff}), which in turn produces an enhance on the apparent diffusion coefficient overcoming the molecular diffusion coefficient ($D_{app} > \bar{D}$).

5. Conclusions

In this study, a thorough analysis of kinetic sorption of Cr(VI) into a solvent impregnated porous microspheres is provided. Polymeric microspheres from PSf and SAN impregnated with Aliquat solvent were prepared and tested for Cr(VI) sorption. Different theoretical models were tested to interpret the Cr(VI) kinetic sorption. Even though the Elovich equation and the pseudo-second order model give satisfactory correlations with the experimental data, we found out that the Crank model is more realistic and appropriate to interpreted our Cr(VI) kinetic sorption results. From this model, it can be seen that there is a surface diffusion contribution to the overall Cr(VI) mass transport

inside the MS which becomes more important when the MS pore size decreases. While the D_{eff} values are in the range of 10^{-15} to 10^{-16} m^2/s, D_s remarkable increases as the MS pore size decreases. This could justify the higher D_{app} values compared with the molecular diffusion coefficient ($\bar{D}$) when the SAN–PVP 1:1 and 1:3 impregnated microsphere are used. A more detailed discussion of the effect of MS material on the sorption capacity and on diffusional parameters is difficult to carry on due to the fact that MS obtained from different polymeric materials have different morphological and/or structural characteristics (porosity, pore size distribution, particle size distribution).

References

[1] C.O. Illanes, N.A. Ochoa, J. Marchese, C. Basualto, F. Valenzuela, Preparation and characterization of polymeric microspheres for Cr(VI) recuperation, Sep. Purif. Technol. 52 (2006) 39–45.

[2] M.P. Gonzalez, I. Saucedo, R. Navarro, M. Avila, E. Guibal, Selective separation of Fe(III), Cd(II), and Ni(II) from dilute solutions using solvent-impregnated resins, Ind. Eng. Chem. Res. 40 (2001) 6004–6013.

[3] R.S. Juang, J.-Y. Su, Sorption of copper and zinc from aqueous sulfate solutions with bis(2-ethylhexyl)phosphoric acid impregnated macroporous resin, Ind. Eng. Chem. Res. 31 (1992) 2774–2779.

[4] N. Kabay, M. Arda, B. Saha, M. Streat, Removal of Cr(VI) by solvent impregnated resins (SIR) containing aliquat 336, React. Funct. Polym. 54 (2003) 103–115.

[5] J.S. Kim, J.C. Park, J. Yi, Zinc ion removal from aqueous solutions using modified silica impregnated with 2-ethyl 2-ethlyhexyl phosphonic acid, Sep. Sci. Technol. 35 (2000) 1901–1916.

[6] J. Serarols, J. Poch, I. Villaescusa, Expansion of adsorption isotherms into equilibrium surface case 1: solvent impregnated resins (SIR), React. Funct. Polym. 48 (2001) 37–51.

[7] E. Kamio, M. Matsumoto, K. Kondo, Extraction mechanism of rare metals with microcapsules containing organophosphorus compounds, J. Chem. Eng. Jpn. 35 (2002) 178–185.

[8] E. Kamio, K. Kondo, Separation of rare metals ions by a column packed with microcapsules containing an extractant, Ind. Eng. Chem. Res. 41 (2002) 3669–3675.

[9] E. Kamio, M. Matsumoto, F. Valenzuela, K. Kondo, Sorption behavior of Ga(III) and In(III) into a microcapsule containing long-chain alkylphosphonic acid monoester, Ind. Eng. Chem. Res. 44 (2005) 2266–2272.

[10] S. Nishihama, G. Nishimura, Hirai, I. Komasawa, Separation and recovery of Cr(VI) from simulated plating waste using microcapsules containing quaternary ammonium salt extractant and phosphoric acid extractant, Ind. Eng. Chem. Res. 43 (2004) 751–757.

[11] M. Rao, A.K. Gupta, Ion exchange process accompanied by ionic reactions, Chem. Eng. J. 24 (1982) 181–190.

[12] J.L. Cortina, N. Miralles, Kinetics studies of heavy metals ions removal by impregnated resins containing di(2,4,4-trimethylpentyl)phosphinic acid, Solvent Extr. Ion Exch. 15 (1997) 1067–1083.

[13] R.-S. Juang, M.-L. Chen, Application of the Elovich equation to the kinetics of metal sorption with solvent-impregnated resins, Ind. Eng. Chem. Res. 36 (1997) 813–820.

[14] W. Rudsinksi, P. Panczyck, in: J.A. Schwarz, C.I. Contescu (Eds.), Surfaces of Nanoparticles and Porous Materials, Dekker, New York, 1998.

[15] R.J. Atkinson, A.M. Posner, J.P. Quirk, Kinetics of isotopic exchange of phosphate at the α-FeOOH-aqueous solution interface, J. Inorg. Nucl. Chem. 34 (1972) 2202–2211.

[16] J. Zhang, R. Stanforth, Slow adsorption reaction between arsenic species and Goethite (α-FeOOH): diffusion or heterogeneous surface reaction control, Langmuir 21 (2005) 2895–2901.

[17] R.-S. Juang, T.-C. Chou, Sorption kinetics of citric acid from aqueous solutions by macroporous resins containing a tertiary amine, J. Chem. Eng. Jpn. 29 (1996) 146–151.

[18] S.L. Lo, S.F. Shine, Recovery of Cr(VI) by quaternary ammonium compounds, Water Res. 32 (1998) 174–178.

[19] G. Parravano, M. Boudart, in: W.G. Frankenburg, V.I. Komarewsky, E.K. Rideal (Eds.), Advances in Catalysis, vol.7, Academic Press, New York, 1955.

[20] A. Pavlatou, N.A. Polyzopoulos, The role of diffusion in the kinetics of phosphate desorption: the relevance of the Elovich equation, J. Soil Sci. 39 (1988) 425–436.

[21] C. Aharoni, D.L. Sparks, S. Levinson, I. Ravina, Kinetics of soil reactions: relationships between empirical equations and diffusion models, Soil Sci. Soc. Am. J. 55 (1991) 1307–1312.

[22] Y.-S. Ho, G. McKay, Pseudo-second order model for sorption proceses, Process Biochem. 34 (1999) 451–465.

[23] A.P. Matthews, W.J. Weber, Effects of external mass transfer and intraparticle diffusion on adsorption rates in slurry reactors, AIChE J. 73 (1976) 91–107.

[24] K.K.H. Choy, G. McKay, Sorption of cadmium, copper and zinc ions onto bone char using Crank diffusion model, Chemosphere 60 (2005) 1141–1150.

[25] J. Crank, The Mathematics of Diffusion, 2nd ed., Oxford University Press, 1979.

[26] C. Aharoni, F.C. Tompkins, Kinetics of adsorption and desorption and the Elovich equation, in: D.D. Eley, P. Pines, P.B. Weisz (Eds.), Advances in Catalysis and Related Subjects, vol. 21, Academic Press, New York, 1970.

[27] D.M. Smith, W.F. Welch, J.A. Jassim, A.R. Chughtai, D.M. Stedman, Shoot-ozone reaction kinetics: spectroscopic and gravimetric studies, Appl. Spectrosc. 42 (1988) 1473–1482.

[28] B. Saha, R.J. Gill, D.G. Bailey, N. Kabay, M. Arda, Sorption of Cr(VI) from aqueous solution by Amberlite XAD-7 resin impregnated with Aliquat 336, React. Funct. Polym. 60 (2004) 223–244.

[29] T. Furusawa, J.M. Smith, Fluid-particle intraparticle mass transport rates in slurries, Ind. Eng. Chem. Fundam. 12 (1973) 197–203.

[30] R.C. Reid, J.M. Prausnitz, B.E. Poling, The Properties of Gases and Liquids, 4th ed., McGraw Hill, 1987.

[31] J.-H. Koh, P.C. Wankat, N.-H.L. Wang, Pore and surface diffusion and bulk-phase mass transfer in packed and fluidized beds, Ind. Eng. Chem. Res. 37 (1998) 228–239.

[32] D.S. Grzegorczyk, G. Carta, Adsorption of amino acids on porous polymeric adsorbents. II. Intraparticle mass transfer, Chem. Eng. Sci. 5 (1996) 819–826.

[33] L.E. Weaver Jr., G. Carta, Protein adsorption on cation exchangers: comparison of macroporous and gel-composite media, Biotechnol. Prog. 12 (1996) 342–355.

[34] P. Li, A.K. Sengupta, Intraparticle diffusion during selective sorption of trace contaminants: the effect of gel versus macroporous morphology, Environ. Sci. Technol. 34 (2000) 5193–5200.

[35] J.S. Mackie, P. Meares, The diffusion of electrolytes in a cation exchange resin membrane, Proc. R. Soc. (Lond.) 232 (1955) 498–509.